

Nonlinear Model Predictive Path Following for an Unmanned Surface Vehicle

1st Xiang Zheng

*Institute of Logistics Science and Engineering
Shanghai Maritime University
Shanghai, China
xiangzheng@shmtu.edu.cn*

2nd Jianhua Wang

*Institute of Logistics Science and Engineering
Shanghai Maritime University
Shanghai, China
jhwang@shmtu.edu.cn*

3rd Shanjia Zhang

*Institute of Logistics Science and Engineering
Shanghai Maritime University
Shanghai, China*

4th Cheng Zhang

*Institute of Logistics Science and Engineering
Shanghai Maritime University
Shanghai, China*

Abstract—This paper presents a two-level nonlinear model prediction control (NMPC) approach for autonomous path following control of under-actuated unmanned surface vehicles with constraints. It performs proper path replanning by taking into consideration of the dynamic constraints and input constraints of the USV in the high-level NMPC, and low-level NMPC solves the control inputs for the USV to follow the new path. The results show that the proposed two-level NMPC approach is able to reduce the change rate of control and avoid excessive control inputs compared with one-level NMPC approach, and the average computation time for each iteration is reduced, which indicates that two-level NMPC approach is more promising for real-time implementation.

Index Terms—unmanned surface vehicle, under-actuated, nonlinear MPC, path following

I. INTRODUCTION

Nowadays unmanned surface vehicles (USVs) have found more and more applications in marine operations for scientific studies, civilian services and military missions. To this effect, it requires USVs to be capable of following the desired path precisely in uncertain environment.

Path following control is a well studied problem. USVs are generally designed small and underactuated for good mobility and energy-saving purposes. Promising solutions have been presented for path following problems of under-actuated surface vessels due to development in nonlinear control and control of under-actuated systems ([2], [4], [6], [7]). However, few have explicitly taken the physical constraints into account, rather they have to achieve constraint enforcement through numerical simulations and trial and error tuning of control parameters.

In real implementations, constraints including the dynamics constraints, under-actuation of the vehicle, and inputs and states constraints, that naturally arise will inevitably degrade the performance of the control system. For example, the thrusts provided by propellers of the USV are limited and excessive actuation is damaging to the propellers. So non-smooth paths, e.g. paths described by straight lines joining way points, that doesn't take enough account of the physical constraints of

the vehicle, is difficult for under-actuated vehicles to follow, and it may result in undesirable jerky, non-continuous motion with high turning rates [3]. In this way, proper path planning that takes into account the constraints of the system becomes necessary in order to alleviate the above problem.

Model Predictive Control (MPC) is viewed as an excellent tool for precise trajectory/path planning in autonomous vehicle guidance. Nonlinear MPC (NMPC) can take into account the full nonlinearity of the model and enforce the constraints in the problem formulation. Furthermore, it is able to handle the multi-objective under-actuated path following problem by combining all the objectives into a single objective function. However, the implementation of NMPC techniques is still limited due to high computational demand associated with online optimization. A new MPC based methodology is proposed in [8], which is based on linear dynamic model and has line-of-sight path generation capability for a way-point tracking of a under-actuated surface vessel with input constraints that simultaneously designed the guidance and control systems. Wang et al. [9] presented the design of an NMPC for a four-control-input boat with control input constraints and the experiments in real environments with a code generation strategy that improves the efficiency of computation. Gao [5] presented a hierarchical approach for MPC based autonomous trajectory tracking and obstacle avoidance of ground autonomous vehicles for reduced computing complexity and better performance.

This paper investigates the hierarchical NMPC scheme for non-smooth path following control of the USV. At the high-level, the NMPC local path replanner, designed based on a simplified model, generates a new reference path that takes into account the kinematic and dynamic constraints of the system, and at the low-level, the low-level NMPC controller computes the vehicle inputs to follow the new path based on a more accurate nonlinear vehicle model. The hierarchical decomposition of the control problem relieves the computational burden of the online optimization of NMPC and the control inputs as well as its change rate are reduced.

The rest of the paper is organized as follows: in the second section, the kinematic and dynamic model of the USV and the path following problem is presented. The formulation of the two-level NMPC problem including high-level path planning and low-level path following for the USV is presented in section 3. Simulation results are presented and analyzed in section 4. The final section is the conclusion.

II. USV MODEL AND PATH FOLLOWING ERROR DYNAMICS

A. USV model

This paper considers a catamaran USV, as shown in Figure 1. Two propellers with fixed orientation are installed at the stern of each hull, thus only two independent thrust forces are generated, which can be decomposed into common and differential modes. Assuming that the vehicle motion is restricted to the horizontal plane, we reduce the degrees of freedom (DOF) of the vehicle model to motions in surge, sway and yaw only by neglecting the heave, roll and pitch modes. Two reference frames are considered: the earth-fixed frame $O_E X_E Y_E$ and the body-fixed frame $O_b X_b Y_b$. For the earth-fixed frame, the origin O_E may be located anywhere on the sea level, axis $O_E Y_E$ is directed to north and axis $O_E X_E$ is directed to east. For the body fixed frame, the origin O_b is attached at the center of gravity of the USV, $O_b X_b$ is the longitudinal axis directed from aft to fore, and $O_b Y_b$ is the transverse axis directed to starboard.



Fig. 1. The "Haixiang" catamaran unmanned surface vehicle

A simplified three degrees of freedom horizontal model is considered that all off-diagonal terms of mass and damping matrices are ignored, as the vessel has port-starboard symmetry and the off-diagonal terms are normally small compared to the main diagonal terms. Moreover, environmental disturbances induced by waves, wind and ocean currents are ignored. Denote $\eta = [x \ y \ \psi]^T$ the vector of position and orientation in the inertial frame, $v = [u \ v \ r]^T$ the velocity vector in the body frame, and $\tau = [\tau_u \ 0 \ \tau_r]^T$ the actuation vector, in which x and y are the positions, ψ is the yaw angle, u , v and r are the velocities of surge, sway and yaw, τ_u is the surge force and τ_r is the yaw moment. Since the sway control force is not available, the model is underactuated. The kinematic equations of the vehicle is given by

$$\dot{\eta} = \mathbf{J}(\eta)v \quad (1)$$

where $\mathbf{J}(\eta)$ is the transformation matrix from body frame to inertial frame

$$\mathbf{J}(\eta) = \begin{pmatrix} \cos \psi & -\sin \psi & 0 \\ \sin \psi & \cos \psi & 0 \\ 0 & 0 & 1 \end{pmatrix} \quad (2)$$

The generalized equation of motion for the dynamics of the USV is written as

$$\mathbf{M}\dot{v} + \mathbf{C}(v)v + \mathbf{D}v = \tau \quad (3)$$

in which \mathbf{M} is the sum of the vehicle mass and added mass matrix

$$\mathbf{M} = \text{diag}\{m_{11}, m_{22}, m_{33}\} \quad (4)$$

and $m_{11} = m - X_{\dot{u}}$, $m_{22} = m - Y_{\dot{v}}$, $m_{33} = I_z - N_{\dot{r}}$, where m is the vehicle mass, I_z is the moment of inertia of the vehicle about the $O_b Z_b$ axis. \mathbf{C} is the matrix of coriolis and centripetal terms and can be written as

$$\mathbf{C}(v) = \begin{pmatrix} 0 & 0 & -m_{22}v \\ 0 & 0 & m_{11}u \\ m_{22}v & -m_{11}u & 0 \end{pmatrix} \quad (5)$$

The damping matrix \mathbf{D} , which are mainly caused by skin friction and wave resistance, is represented by linear damping terms with the nonlinear terms ignored

$$\mathbf{D}(v) = \begin{pmatrix} X_u & 0 & 0 \\ 0 & Y_v & 0 \\ 0 & 0 & N_r \end{pmatrix} \quad (6)$$

The surge force and yaw moment are the common and differential modes of the two thrust forces, F_L and F_R , from the left propeller and right propeller respectively

$$\tau_u = F_L + F_R \quad (7)$$

$$\tau_r = \frac{d}{2}(F_R - F_L) \quad (8)$$

where d is the distance between the propellers. Manoeuvres can be obtained by change both the thrust forces to make the vessel turn as required whilst maintaining the average force at all times.

B. Path following error dynamics

For unmanned surface vehicles operating in the open sea, the path is often straight line or way-point path, which consists of piecewise straight lines. We consider a generic desired path composed of a set of way-points $(..., P_{k-1}, P_k, P_{k+1}, ...)$. P_k is the current way point with P_{k-1} being its previous way-point and P_{k+1} being the next way-point. When the vessel is within a circle of radius R_k of the current way-point, it switches to the next way-point at P_{k+1} . The path following error dynamics based on Serret-Frenet equations for path of straight lines is given as follows

$$\Delta \dot{h} = u \sin(\bar{\psi}) + v \cos(\bar{\psi}) \quad (9)$$

$$\Delta \dot{\psi} = r \quad (10)$$

where Δh is the cross-track error defined as the distance between the center of gravity of the vessel O_b and the path.

$\Delta\bar{\psi} = \psi - \psi_p$ is the relative heading error with respect to the path direction. ψ is the heading angle of the vessel and ψ_p is the path direction, N is the unit normal vector of the path and T is the unit vector in the path direction, as shown in Fig 2. Path following control acts on the USV's orientation to drive it to the path, i.e. drive both Δh and $\Delta\bar{\psi}$ to zero, while the vehicle's surge speed tracks a desired profile [1].

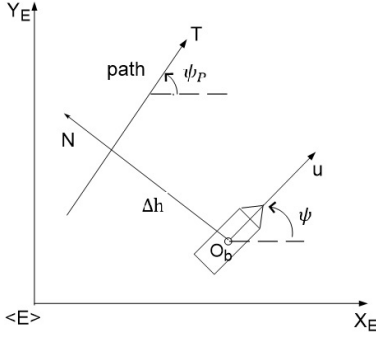


Fig. 2. Schematic representation of variables for a straight-line path following

III. TWO-LEVEL NMPC FORMULATION FOR PATH FOLLOWING CONTROL

Nonlinear model predictive (NMPC) is a control strategy that determines the control action at each sampling instant by solving online an optimization problem over a horizon based on model prediction for feedback control of nonlinear systems. MPC has outstanding advantages over other control strategies for its ability of dealing with multi-objective controller design and handling constraints, and it has been widely used in process industry. However, the implementation of NMPC for systems with fast and nonlinear dynamics is still fundamentally limited due to the computational complexity associated with its iterative online optimization.

This section presents the two-level NMPC formulation for both path replanning and path following. The architecture of the control scheme is shown in Fig. 3. We consider the case of non-smooth way-point path as the desired path. The desired path $[0, \psi_p]$ is fed to the high-level path replanner. The path replanner replans the path using a simplified model of the vehicle. The replanned path $[\Delta h_{ref}, \psi_{ref}]$ is then fed to the low-level path following controller. The replanned path $[\Delta h_{ref}, \psi_{ref}]$ is then fed to the low-level path following controller.

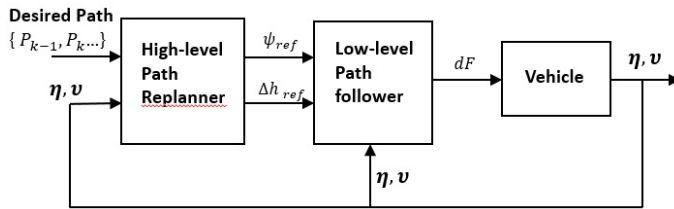


Fig. 3. Architecture of two-level NMPC scheme

The path following controller computes the optimal input to follow the new path using a more accurate model. For

simplicity, we assume that the states of the system are available for measurement. The surge speed u is constant, hence the surge force τ_u is constant and the thrusts of the left and right propellers can be expressed as follows

$$F_L = F_b - dF \quad (11)$$

$$F_R = F_b + dF \quad (12)$$

where F_b is constant, and dF is to be solved by the controller to produce the yaw moment needed to drive the USV to follow the desired path. An error model combining the path following error dynamics represented by Eq. (9) and the dynamic model of the USV represented by Eq. (3) can be written into the following compact form

$$\dot{\mathbf{x}} = \mathbf{f}(\mathbf{x}, dF) \quad (13)$$

where $\mathbf{x} = [\Delta h \ \bar{\psi} \ v \ r]$. To formulate the NMPC controller, the model described by (13) is discretized with a sampling time t_s

$$\mathbf{x}(k+1) = \mathbf{f}_d(\mathbf{x}(k), dF(k)) \quad (14)$$

$$dF(k) = dF(k-1) + \Delta dF(k) \quad (15)$$

in which the change rate of control input, ΔdF , is used as optimization variable.

Two NMPC problems are formulated for the high-level path replanning and for the low-level path following. The two problems can be set up with different sampling time, prediction horizon and control horizon.

A. High-level path replanner

The high-level MPC for path replanning is based on a simplified model to reduce the derivation. The states of the model is chosen as $\mathbf{x} = [\Delta h \ \bar{\psi} \ r]$ with the assumption that $|v/u| \ll 1$. The path replanner is formulated as follows

$$\min_{\Delta dF} \sum_{j=1}^{N_{p1}} \mathbf{x}_{k+j}^T Q_H \mathbf{x}_{k+j} + \Delta dF_{k+j-1}^T R_H \Delta dF_{k+j-1} \quad (16)$$

subject to

$$\mathbf{x}(k+j) = \mathbf{f}_d(\mathbf{x}(k+j-1), dF(k+j-1)) \quad j = 1, 2, \dots, N_{p1} \quad (17)$$

$$\Delta dF_{k+j} = dF_{k+j} - dF_{k+j-1} \quad j = 1, 2, \dots, N_{c1} \quad (18)$$

$$\Delta dF_{k+j-1} = 0 \quad j = N_{c1} + 1, \dots, N_{p1} \quad (19)$$

$$dF_{min} \leq dF_{k+j-1} \leq dF_{max} \quad j = 1, 2, \dots, N_{p1} \quad (20)$$

$$\Delta dF_{min} \leq \Delta dF_{k+j-1} \leq \Delta dF_{max} \quad j = 1, 2, \dots, N_{c1} \quad (21)$$

in which N_{p1} and N_{c1} are the prediction horizon and control horizon respectively, and Q_H and R_H are the weighting matrices. The computational complexity of the optimization is reduced by holding the last $N_p - N_c$ inputs dF_{k+j} constant. The cost function penalizes the deviation of the predicted path from the reference path and the control inputs.

B. Low-level NMPC controller

The low-level NMPC for path following control is based on the more accurate model with states $\mathbf{x} = [\Delta h \ \psi \ v \ r]$. The path follower aims to track the replanned path provided by the high-level path replanner. The problem is formulated as follows

$$\min_{\Delta dF} \sum_j^{N_{p2}} (\mathbf{x}_{k+j} - \mathbf{x}_{k+j}^{ref})^T Q_L (\mathbf{x}_{k+j} - \mathbf{x}_{k+j}^{ref}) + \Delta dF_{k+j-1}^T R_L \Delta dF_{k+j-1} \quad (22)$$

subject to

$$\mathbf{x}(k+j+1) = f_d(\mathbf{x}(k+j), dF(k+j-1)) \quad j = 1, \dots, N_{p2} \quad (23)$$

$$\Delta dF_{k+j} = dF_{k+j} - dF_{k+j-1} \quad j = 1, \dots, N_{c2} \quad (24)$$

$$\Delta dF_{k+j-1} = 0 \quad j = N_{c1} + 1, \dots, N_{p2} \quad (25)$$

$$dF_{min} \leq dF_{k+j-1} \leq dF_{max} \quad j = 1, \dots, N_{p2} \quad (26)$$

$$\Delta dF_{min} \leq \Delta dF_{k+j-1} \leq \Delta dF_{max} \quad j = 1, \dots, N_{c2} \quad (27)$$

in which N_{p2} and N_{c2} are the prediction horizon and control horizon respectively, and Q_L and R_L are the weighting matrices. The cost function penalizes the deviation of the state from the replanned reference state and the control input.

IV. SIMULATION RESULTS AND DISCUSSION

In this section, the performance of the two-level NMPC for guidance and path following control of the USV is evaluated in simulation by drawing a comparison with a one-level NMPC for path following. The parameters of the model of the USV including the main geometric dimension parameters and hydrodynamic coefficients are presented in Table 1. The values are used mainly with the purpose to simulate the capability of the path following controller. The model is discretized with a sampling time $t_s = 0.06s$. It assumes that the surge speed of the USV is kept at $0.6m/s$. Three way-points are set as $P_1 = (0, 0)$, $P_2 = (20, 0)$, $P_3 = (20, 40)$. The desired path are the straight lines connecting two adjacent way-points. The initial position and heading of the USV is set at $(0, -5)$ and $-\pi/2$, so the initial cross track error is $5m$. For the two-level NMPC, the prediction horizons are set as $N_{p1} = N_{p2} = 20$, and the control horizons are set as $N_{c1} = N_{c2} = 8$. The weighting matrices are set as $Q_H = diag(3, 1, 0.1)$, $Q_L = diag(3, 1, 0, 0.1)$ and $R_H = R_L = 0.00001$. The constraints for the thrusts from the left and right propellers are set as $-80N \leq F_L, F_R \leq 80N$, and in consequence we have the constraint $-80N \leq dF \leq 50N$. The change rate of the forces are set to be limited to $-2N \leq \Delta dF \leq 2N$ that the USV will be able to accelerate to full surge speed in $3s$. These constraints are very important because the control signals can easily require the propellers operate at their limit during transition and frequent large control increments often cause adverse effects on motors as well as on maneuvering performance and stability of the USV as they may induce large roll motion in reality.

Figures 4-7 presents results of the two-level NMPC in comparison with one-level NMPC for the following of the straight way-point paths, the parameters of the one-level NMPC based on a more accurate model are set as the same as the low-level NMPC. figure 4 and figure 5 show that both control strategies achieve satisfactory path following performance generating smooth trajectories of the USV, and the two-level NMPC achieves slightly faster convergence to the desired path. In figure 6 and figure 7, it can be seen that the control inputs and their change rates are within the limits imposed by the constraints. The maximum control forces for the two-level NMPC is smaller than the one-level NMPC, and the change rate of control forces of the two-level NMPC are considerably smaller than one-level NMPC. This indicates that the two-level NMPC is much better in avoiding excessive input changes, this is due to the decomposition of the optimization based control problem with the hierarchical architecture of the two-level NMPC scheme. Figure 8 shows the CPU time needed to determine the next control action. With NMPC method, it is critical to make sure that the computation time needed for each control action is smaller than the sampling time $t_s = 0.06s$. It is noted that this threshold has been exceeded around the turning region of the path, while the two-level NMPC used less computation time than the one-level NMPC. The average CPU time per iteration are $0.0261s$ for the one-level NMPC and $0.0259s$ for the two-level NMPC.

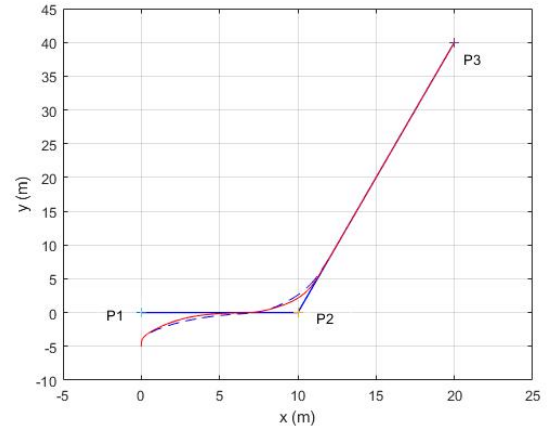


Fig. 4. Trajectory of the USV with two-level NMPC (solid line) and one-level NMPC (dashed line) path following control

TABLE I
USV PARAMETERS FOR SIMULATION

Mass, m	60kg
Dimension, ($L \times W \times H$)	$1.6m \times 1.2m \times 0.36m$
Inertia, I_z	$20kgm^2$
m_{11}	67.37
m_{22}	91.87
m_{33}	34
X_u	100
Y_v	100
N_r	150

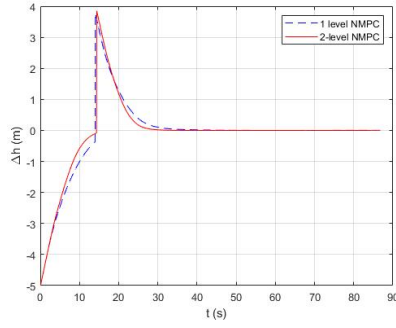


Fig. 5. Cross tracking error Δh for the two-level NMPC and one-level NMPC schemes

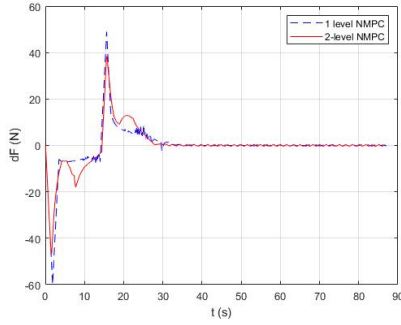


Fig. 6. Control forces for the two-level NMPC and one-level NMPC schemes

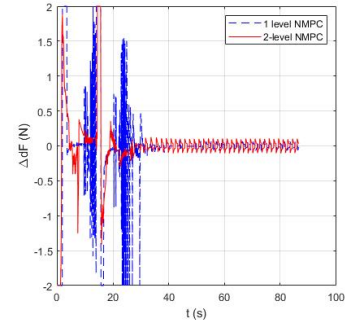


Fig. 7. Change rate of control force ΔdF for the two-level NMPC and one-level NMPC schemes

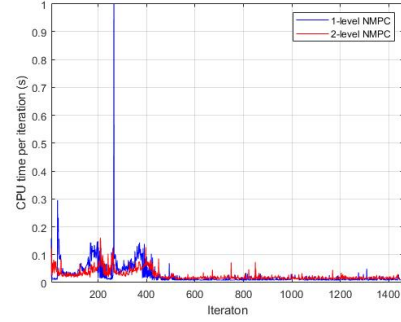


Fig. 8. CPU time per iteration for the two-level NMPC and one-level NMPC schemes

V. CONCLUSION

In this paper, a two-level NMPC approach for path following of the USV with constraints is presented. Straight line waypoint paths are considered and the path-following problem is formulated with the dynamic model of the USV combined with the path-following error dynamic model. The high-level NMPC path planner replans the path taking into consideration of dynamic constraints and input constraints of the USV, and the low-level NMPC controller computes the vehicle inputs to follow the new path. The simulation results show that the proposed two-level approach achieves satisfactory path following and successfully reduces the control inputs. It is by decomposing the control problem into two hierarchical parts that the computing complexity of each parts are substantially reduced.

Future work will take obstacle avoidance into consideration at the high-level, and both the advantages and limitations of the two-level NMPC scheme will be further analyzed in terms of its ability of reducing computing complexity and improving the stability and robustness of the system.

REFERENCES

- [1] Marco Bibuli, Gabriele Bruzzone, Massimo Caccia, and Lionel Lapierre. Path-following algorithms and experiments for an unmanned surface vehicle. *Journal of Field Robotics*, 26(8):669–688, 2009.
- [2] M. Breivik and T. Fossen. Path following of straight lines and circles for marine surface vessels. *Proceeding of the 6th IFAC CAMS*, 37(10):65–70, 2004.

- [3] S. Campbell, W. Naeem, and G. W. Irwin. A review on improving the autonomy of unmanned surface vehicles through intelligent collision avoidance manoeuvres. *Annual Reviews in Control*, 36(2012):267–283, 2012.
- [4] K. Do and J. Pan. Underactuated ships follow smooth paths with integral actions and without velocity measurements for feedback: theory and experiments. *IEEE transactions on control systems technology*, 14(2):308–322, 2006.
- [5] Yiqi Gao. Model predictive control for autonomous and semiautonomous vehicles. *Theses - University of California, Berkeley*, 2014.
- [6] Zhen Li, Jing Sun, and Soryeok Oh. A robust nonlinear control design for path following of a marine surface vessel. *IFAC conference on control applications in marine systems*, 40(17):99–104, 2007.
- [7] Zhen Li, Jing Sun, and Soryeok Oh. Design, analysis and experimental validation of a robust nonlinear path following controller for marine surface vessels. *Automatica*, 45(2009):1649–1658, 2009.
- [8] So-Ryeok Oh and Jing Sun. Path following of underactuated marine surface vessels using line-of-sight based model predictive control. *Ocean Engineering*, 37(2010):29–38, 2010.
- [9] Wei Wang, Luis A. Mateos, Shinkyu Park, Pietro Leoni, and Banti Gheneti. Design, modeling, and nonlinear model predictive tracking control of a novel autonomous surface vehicle. In *IEEE International Conference on Robotics and Automation*, pages 6189–6196, 2018.